Light scattering by an array of electric and magnetic nanoparticles

Braulio García-Cámara[1, 2*], Fernando Moreno[1], Francisco González[1] and Olivier J. F. Martin [2]

[1]*Grupo de Óptica. Departamento de Física Aplicada. Universidad de Cantabria, Avd. de los Castros s/n, 39005, Santander, Spain*
[2] *Nanophotonics and Metrology Laboratory, Ecole Polytechnique Fédérale de Lausanne (EPFL), 1015 Lausanne, Switzerland*
*garciacb@unican.es

Abstract: Light scattering by an array of alternating electric and magnetic nanoparticles is analyzed in detailed. Specific geometrical conditions are derived, where such an array behaves like double-negative particles, leading to a suppression of the backscattered intensity. This effect is very robust and could be used to produce double-negative metamaterials using single-negative components.

OCIS codes: (290.1350) Backscattering; (160.3918) Metamaterials; (160.4236) Nanomaterials.

References and links

1. P. K. Jain, X. Huang, I. H. El-Sayed, and M. A. El-Sayed, "Noble metals on the nanoscale: optical and photothermal properties and some applications in imaging, sensing, biology, and medicine," Acc. Chem. Res. **41**(12), 1578–1586 (2008).
2. X. Liu, and Q. Huo, "A washing-free and amplification-free one-step homogeneous assay for protein detection using gold nanoparticle probes and dynamic light scattering," J. Immunol. Methods **349**(1-2), 38–44 (2009).
3. K. R. Catchpole, and A. Polman, "Plasmonic solar cells," Opt. Express **16**(26), 21793–21800 (2008).
4. S. Kawata, Y. Inouye, and P. Verma, "Plasmonics for near-field nano-imaging and superlesing," Nat. Photonics **3**(7), 388–394 (2009).
5. M. Guillaumée, L. A. Dunbar, Ch. Santschi, E. Grenet, R. Eckert, O. J. F. Martin, and R. P. Stanley, "Polarization sensitive silicon photodiodes using nanostructured metallic grids," Appl. Phys. Lett. **94**(19), 193503 (2009).
6. H. Lee, Z. Liu, Y. Xiong, C. Sun, and X. Zhang, "Development of optical hyperlens for imaging below the diffraction limit," Opt. Express **15**(24), 15886–15891 (2007).
7. E. S. Day, J. G. Morton, and J. L. West, "Nanoparticles for thermal cancer therapy," J. Biomech. Eng. **131**(7), 074001–074005 (2009).
8. S. S. Acimovic, M. P. Kreuzer, M. U. González, and R. Quidant, "Plasmon Near-Fields Coupling in Metal Dimers as a Step toward Single-Molecule Sensing," Nano Lett. **3**, 1231–1237 (2009).
9. M. Kerker, D.-S. Wang and C.L. Giles, "Electromagnetic scattering by magnetic particles," J. Opt. Soc. Am **73**, 765–767 (1983).
10. B. García-Cámara, J. M. Saiz, F. González, and F. Moreno, "Nanoparticles with unconventional scattering properties: Size effects," Opt. Commun. **283**(3), 490–496 (2010).
11. N. Engheta, "Circuits with light at nanoscales: optical nanocircuits inspired by metamaterials," Science **317**(5845), 1698–1702 (2007).
12. D. R. Smith, J. B. Pendry, and M. C. K. Wiltshire, "Metamaterials and negative refractive index," Science **305**(5685), 788–792 (2004).
13. V. Shalaev, "Optical negative-index metamaterial," Nat. Photonics **1**(1), 41–48 (2007).
14. A. Christ, O. J. F. Martin, Y. Ekinci, N. A. Gippius, and S. G. Tikhodeev, "Symmetry breaking in a plasmonic metamaterial at optical wavelength," Nano Lett. **8**(8), 2171–2175 (2008).
15. J. B. Pendry, "Negative refraction makes a perfect lens," Phys. Rev. Lett. **85**(18), 3966–3969 (2000).
16. N.-H. Shen, S. Foteinopoulou, M. Kafesaki, T. Koschny, E. Ozbay, E. N. Economou, and C. M. Soukoulis, "Compact planar far-field superlens based on anisotropic left-handed metamaterials," Phys. Rev. B **80**(11), 115123–115131 (2009).
17. J. B. Pendry, D. Schurig, and D. R. Smith, "Controlling electromagnetic fields," Science **312**(5781), 1780–1782 (2006).
18. C. L. Holloway, E. F. Kuester, J. Baker-Jarvis, and P. Kabos, "A double negative (DNG) composite medium composed of magnetodielectrc spherical particles embedded in a matrix," IEEE Trans. Antenn. Propag. **51**(10), 2596–2603 (2003).
19. B. García-Cámara, F. Moreno, F. González, J. M. Saiz, and G. Videen, "Light scattering resonances in small particles with electric and magnetic properties," J. Opt. Soc. Am. A **25**(2), 327–334 (2008).

20. B. García-Cámara, F. González, F. Moreno, and J. M. Saiz, "Exception for the zero-forward scattering theory," J. Opt. Soc. Am. A **25**(11), 2875–2878 (2008).
21. C. L. Holloway, M. A. Mohamed, E. F. Kuester, and A. Dienstfrey, "Reflection and transmission properties of a metalfilm: with an application to a controllable surface composed of resonant particles," IEEE Trans. Electromagn. Compat. **47**(4), 853–865 (2005).
22. N. A. Mirin, and N. J. Halas, "Light-bending nanoparticles," Nano Lett. **9**(3), 1255–1259 (2009).
23. A. Alù, and N. Engheta, "The quest for magnetic plasmons at optical frequencies," Opt. Express **17**(7), 5723–5730 (2009).
24. C. Bohren, and D. Huffman, *Absorption and Scattering of Light by Small Particles* (Wiley, 1983)
25. B. T. Draine, and P. J. Flatau, "Discrete-dipole approximation for scattering calculations," J. Opt. Soc. Am. A **11**(4), 1491–1499 (1994).
26. J. D. Jackson, *Classical Electrodynamics*, (Wiley, 1975).
27. G. W. Mulholland, C. F. Bohren, and K. A. Fuller, "Light Scattering by Agglomerates: Coupled Electric and Magnetic Dipole Method," Langmuir **10**(8), 2533–2546 (1994).
28. P. Chýlek, and R. G. Pinnick, "Nonunitarity of the light scattering approximations," Appl. Opt. **18**(8), 1123–1124 (1979).
29. R. Carminati, J.-J. Greffet, C. Henkel, and J. M. Vigoureux, "Radiative and non-radiative decay of a single molecule close to a metallic nanoparticle," Opt. Commun. **261**(2), 368–375 (2006).
30. N. Liu, L. Langguth, T. Weiss, J. Kästel, M. Fleischhauer, T. Pfau, and H. Giessen, "Plasmonic analogue of electromagnetically induced transparency at the Drude damping limit," Nat. Mater. **8**(9), 758–762 (2009).

1. Introduction

Light scattering by nanostructures and nanoparticles is one of the most promising emerging fields in nanoscience, since it paves the way for many important applications in several areas of biology and medicine (cancer treatments, nanobiosensors, molecular orientation sensing, etc) [1,2] as well as in other technologies such as efficient solar cells, high resolution microscopy, and optical communications [3–5]. The performances of these devices and techniques can be improved by controlling the optical properties of the nanostructures or nanoparticles. For example, the excitation of electromagnetic resonances produces an important enhancement of the scattered intensity which can be used to enhance spectroscopic signals [6], or to destroy cancerous cells [7,8].

Quite a few years ago, M. Kerker et al. proposed that light scattered by a dipole-like particle with specific optical constants can exhibit a directional behaviour [9]. In particular, no scattering occurs in either the backward or forward directions. We have extended this work and demonstrated that a minimum in the scattered light can be observed, under similar conditions for the optical constants, for finite sized particles and for scattering angles different from 0° and 180° [10]. Additional work has focused on the design of nanostructures able to redirect scattered light [11].

The control of the optical properties of structures and, in particular, nanostructures is the motivation for developing, designing and manufacturing metamaterials. These new materials are built up from different internal nanostructures in a way such that effective optical constants are generated. Changing the density, size, shape or composition of the internal nanostructures, modifies the effective optical constants [12]. Efforts in this field have focused on obtaining metamaterials in an as wide as possible part of the electromagnetic spectrum, with a current push toward optical frequencies [13,14]. The unusual scattering properties of metamaterials enable exciting applications such as hyperlensing [6], superlensing [15,16] or electromagnetic cloaking [17]. Also, different configurations of these structured-materials are able to produce simultaneously negative values for the electric permittivity (ε) and the magnetic permeability (μ) [18]. Such materials are called Double-Negative (DNG) and exhibit extremely interesting features. When $\varepsilon<0$ and $\mu<0$, the phase of the wave moves in the opposite direction from the energy flow, hence the name "left-handed" to describe these materials; light refraction in these media is on the "left" side instead of the usual "right" side, this effect is the basis for the perfect lens [15].

In a previous work we have studied light scattered by very small particles with double-negative materials properties [19]. Specific resonances can be excited in these systems (dipolar and quadrupolar resonances, both electric and magnetic), leading to a strong enhancement of the scattered intensity. In particular, materials with permittivity and permeability such that $\varepsilon = \mu = -2$ produce the simultaneous excitation of electric and

magnetic dipolar resonances, producing dramatic values for the scattered intensity. This pair of optical parameters also fulfils *Kerker's conditions* [9] for zero-backward and zero-forward light scattering. The first effect can be observed in this system, but the zero-forward light scattering does not appear due to the strong enhancement caused by the dipolar resonances. For this reason, the pair of optical constants ($\varepsilon = \mu = -2$) represents an exception for the zero-forward condition proposed by M. Kerker *et al.* [20].

Unfortunately, manufacturing a nanoparticle with simultaneously ε and μ negative and equal to *-2* is beyond today's technology. However, C. Holloway *et al.* have demonstrated that an array of magnetodielectric particles embedded in a matrix can exhibit double-negative optical constants [18]. These authors further studied the reflection and transmission properties of these structures [21]. Following these works and the possibility to generate nanoparticles and nanostructures that present magnetic plasmonic resonances [22,23], we present in this paper a theoretical study of an array composed of resonant electric and magnetic particles that exhibit a double-negative behaviour, including a minimum backward scattering amplitude, that we analyse in detail as a function of different geometrical parameters of the array.

The paper is organized as follows: after a brief review of the light scattering theory and the approximations that we have used in section 3, we consider and analyze the polar distributions of the light scattered by different square arrays composed by four particles, electric and/or magnetic, as function of the geometrical characteristics. Design rules are obtained from those small systems. In sections 4 and 5 we use these rules to design and study arrays with a larger number of particles, as well as additional layers. The last section summarizes the main results of the paper.

2. A short review of coupled electric and magnetic dipole method

Light scattering by a homogeneous, isotropic and spherical particle with radius *R* illuminated by a linearly polarized plane wave traveling in the *z*-direction [$\vec{k} = (0,0,k) = (0,0,\omega/c)$, *k* being the wavenumber in the surrounding medium and ω the angular frequency] can be analyzed using the Lorenz-Mie theory [24]. If the particle is very small compared to the incident wavelength (λ), its refractive index is not very large and it is isolated of far from other particles (*D>>R*), light scattering obtained by the Mie theory can be approximated using only the dipolar terms of the multipolar expansion. This approximation is called the Dipolar Approximation (DA) [25]. Under this approach, the polarizabilities of the particle can be expressed, using the Clausius-Mossotti relation [24], as

$$\alpha_E \propto \frac{\varepsilon_p - \varepsilon_m}{\varepsilon_p + 2\varepsilon_m}$$

$$\alpha_H \propto \frac{\mu_p - \mu_m}{\mu_p + 2\mu_m}.$$

(1)

In Eq. (1) α_E and α_H are the electric and magnetic polarizabilities, ε_P and ε_m the electric permittivity of the particle and the surrounding medium and μ_P and μ_m the magnetic permeability of the particle and the surrounding medium, respectively. As can be seen in Eq. (1), in the usual case where $\varepsilon_m = \mu_m = 1$, the scattered intensity by the particle presents a resonance when ε_p and/or μ_p is equal to *-2* [19]. From Eq. (1), we can write the electric ($\vec{p}$) and magnetic ($\vec{m}$) moments as

$$\vec{p} = \varepsilon_0 \alpha_E \vec{E}_0$$

$$\vec{m} = \alpha_H \vec{H}_0 ,$$

(2)

where $\vec{E}_0$ and $\vec{H}_0$ are the electric and magnetic incident fields and ε_0 is the vacuum electric permittivity. The scattered electromagnetic fields can be calculated easily from Eq. (2) [26].

This method has been generalized to calculate the scattered intensity by a group of very small particles, taking into account the possible interactions between them. This approximation for the scattering by agglomerates is known as *Coupled Electric and Magnetic Dipole Method* and was proposed by G. Mulholland *et al.* [27]. This method considers each particle as composed of two dipoles, one electric and one magnetic, each characterized by an electric and a magnetic polarizability according to Eq. (1). The incident electric and magnetic fields ($\vec{E}_0$ and $\vec{H}_0$ in Eq. (2)) at each particle are the sum of the incident electromagnetic field ($\vec{E}_{pw}$ and $\vec{H}_{pw}$) plus the contributions from the other particles. Hence, the electric and magnetic fields at the *ith* particle caused by the *jth* particle are written as

$$\vec{E}_i = \sum_{j\neq i} a_{ij}\alpha_E \vec{E}_j + b_{ij}\alpha_E(\vec{E}_j \cdot \vec{n}_{ji})\vec{n}_{ji} - d_{ij}\left(\frac{\mu_o}{\varepsilon_0}\right)^{1/2}\alpha_H(\vec{n}_{ji}\times\vec{H}_j)$$

$$\vec{H}_i = \sum_{j\neq i} a_{ij}\alpha_H \vec{H}_j + b_{ij}\alpha_H(\vec{H}_j \cdot \vec{n}_{ji})\vec{n}_{ji} - d_{ij}\left(\frac{\varepsilon_o}{\mu_0}\right)^{1/2}\alpha_E(\vec{n}_{ji}\times\vec{E}_j)$$

(3)

where $\vec{n}_{ji}$ is the direction vector from the *jth* particle to the *ith* one, and the coefficient a_{ij}, b_{ij} and d_{ij} are given by [27]

$$a_{ij} = \frac{1}{4\pi}\frac{e^{ikr_{ij}}}{r_{ij}}\left(k^2 - \frac{1}{r_{ij}^2} + \frac{ik}{r_{ij}}\right)$$

$$b_{ij} = \frac{1}{4\pi}\frac{e^{ikr_{ij}}}{r_{ij}}\left(-k^2 + \frac{3}{r_{ij}^2} - \frac{3ik}{r_{ij}}\right)$$

(4)

$$d_{ij} = \frac{1}{4\pi}\frac{e^{ikr_{ij}}}{r_{ij}}\left(k^2 + \frac{ik}{r_{ij}}\right),$$

where r_{ij} is the distance between the two considered particles (*i* and *j*) and $k = 2\pi/\lambda$. Then, the total incident field at the particle *ith* (sum of the incident wave plus Eq. (3)) can be derived, as it is explained in Ref [27], in the following way

$$\begin{pmatrix}\vec{E}_i \\ \vec{H}_i\end{pmatrix} = \begin{pmatrix}\vec{E}_{pw} \\ \vec{H}_{pw}\end{pmatrix}[I - M]^{-1}$$

(5)

M and *I* being the matrix that contains the particles interactions given by coefficients a_{ij}, b_{ij} and d_{ij} and the identity one, respectively. Once known the total local fields, we can propagate it, using the expression of the dipolar moments (Eq. (2)), in order to obtain the scattered field.

This method agrees with Mie calculations very well for the light scattered in the far-field by very small particles [27]. Furthermore, this approach needs only very short computation times, which makes it the method of choice for the systems studied in this paper.

At this point it is important to remark that the dipolar approximation considered for our calculations do not fulfilled the Optical Theorem. The non-unitarity of it forces to use other expressions to calculate the extinction efficiency [28]. A small correction in the polarizabilities, that is the radiative correction [29], can be considered to fulfill the Optical Theorem. However, in our case, we have considered optical properties near the resonant conditions ($\varepsilon = -2$, $\mu = -2$) for which the radiative correction is negligible.

3. Description of the system: geometrical and optical conditions

Using the Coupled Electric and Magnetic Dipole Method (CEMD), described in the previous section, we now analyze the scattering patterns for an aggregate of four spheres forming a

square. Two types of particles are considered, the electric ones with an electric permittivity (ε) equal to *-2.01* and a magnetic permeability $\mu = 1$ and the magnetic ones with $\varepsilon = 1$ and $\mu = -2.01$. These values are chosen because the electric and the magnetic plasmon resonances are still excited and a very high scattered intensity is observed, but we do not produce infinite values for the electric and magnetic polarizabilities, as it would happen if ε or μ were equal to *-2*. Similar results, but with much smaller values for the scattered intensity, can be obtained for arbitrary values for ε and μ, under the condition that the electric permittivity of the electric particles is equal to the magnetic permeability of the magnetic ones. We have used the diagonal of the square to determine the distance between particles. In this case, it is fixed to D = *0.5λ*, while the radius of the particles *is R = 0.01λ*. As can be seen in Fig. 1, different combinations of electric and magnetic particles are analyzed.

The system is illuminated by a plane wave linearly polarized. Both polarizations, with the electric field parallel (P polarization) or normal to the scattering plane (S polarization), are considered. The position of the array of nanoparticles is considered in the scattering plane (left column of Fig. 1) or in a plane normal to the incident direction (right column).When only one particle – either electric or magnetic – is different from the rest of the array (Fig. 1a) and 1b)), the exact location of this different particle does not produce any remarkable changes in the scattering pattern. For this reason, we only report here results produced for one specific location of that different particle.
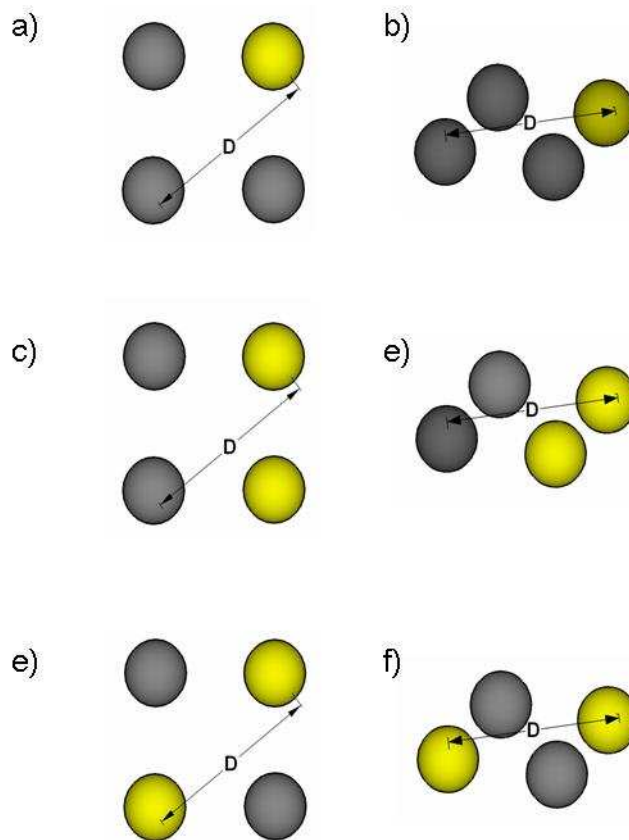

Fig. 1. The different array configurations under study. The dark particles are electric ($\varepsilon = -2.01, \mu = 1$) and the yellow ones are magnetic ($\varepsilon = -2.01, \mu = 1$). Both particles placed on the scattering plane (left column) or on a normal plane (right column) are considered. The particle radius is $R = 0.01\lambda$ and $D = 0.5\lambda$.

In Fig. 2, we show the scattering patterns corresponding to the different geometries indicated in Fig. 1. Some interesting features can be observed. In particular, the scattered intensity presents minima at some scattering directions for specific geometries cases. Let us focus our attention to the cases d) and f) in Fig. 2. These configurations present a sharp minimum in the backward direction and the shape of the scattering pattern is very similar to that for an isolated particle with $\varepsilon = \mu = -2.01$ [20]. This is illustrated in Fig. 3: these two configurations are composed by four particles (two electric and two magnetic) on a plane normal to the incident direction and the magnetic particles are in the corners of the same side and the electric ones in the other side (Fig. 1d) or the electric and magnetic particles are placed alternatively in the square corners (Fig. 1f).

Fig. 2. Scattering patterns, for both incident polarizations, corresponding to the different arrays shown in Fig. 1.

Hence, the electric and magnetic contributions in those cases are compensated in the backward direction, producing a minimum in the field scattered in that direction. Also, as the contribution to the light scattering is similar for the two types of particles, the polar plots are similar for both polarizations. This result indicates that the array configurations described in Fig. 1d) and 1f) scatter like a double negative particle with an electric permittivity equal to

that of the electric particles and a magnetic permeability equal to that of the magnetic particles. This result is similar to that presented by C. Holloway *et al.* [18] but with the difference that the distributions in Fig. 2 exhibit a similar behaviour to the special and very important case where $\varepsilon = \mu = -2.01$, with a double resonant behaviour and a scattering minimum in the backward direction.
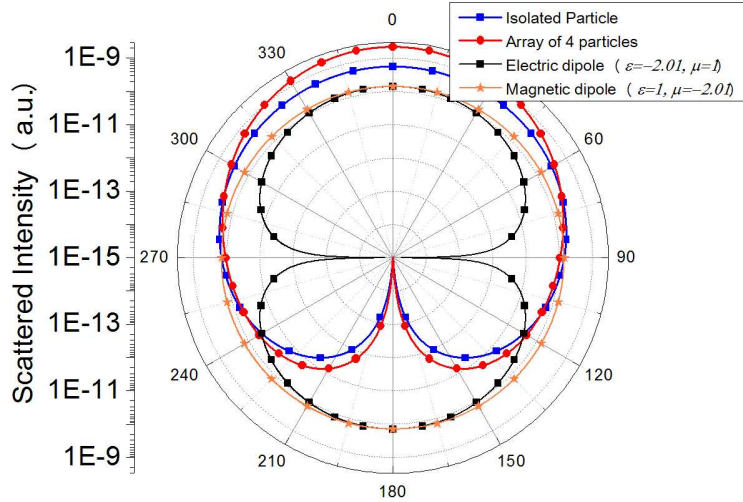

Fig. 3. Comparison of the scattering patterns for an isolated particle ($R = 0.01\lambda$) with optical constants ($\varepsilon = \mu = -2.01$) and for an array of electric ($\varepsilon = -2.01$, $\mu = 1$) and magnetic ($\varepsilon = 1$, $\mu = -2.01$) particles ($R = 0.01\lambda$) with a spatial distribution indicated in Fig. 1f). Also the scattering patterns for an electric ($\varepsilon = -2.01, \mu = 1$) and a magnetic ($\varepsilon = 1$, $\mu = -2.01$) dipole has been included. The incident wave is polarized with the electric field parallel to the scattering plane (P polarization).

The scattering behaviour for both cases described in Fig. 1d) and 1f) changes when the distance between the particles in the array is changed. In Fig. 4, respectively 5, we plot the polar distribution of the scattered intensity for the geometrical configurations shown in Fig. 1d), respectively 1f), for several values for the square diagonal *D*.

While the alternate-configuration (Fig. 1f) exhibits a stable minimum of the scattered intensity in the backward direction when the distance changes, the other configuration (Fig. 1d) does not present this minimum for short distances and, for large distances, the angular range for the minimum scattering is extremely small. Hence, in the following, we only consider the geometrical configuration described in Fig. 1f) which we call "alternate" configuration. In Fig. 5, it can be seen that the inter-particle distance produces a slight change in the angular range at which the minimum scattering is observed. For the two shortest and two largest distances, the minimum backscattering range is around 30° centred on 180°, but for a distance equal to the incident wavelength, this range is increased to 60°.
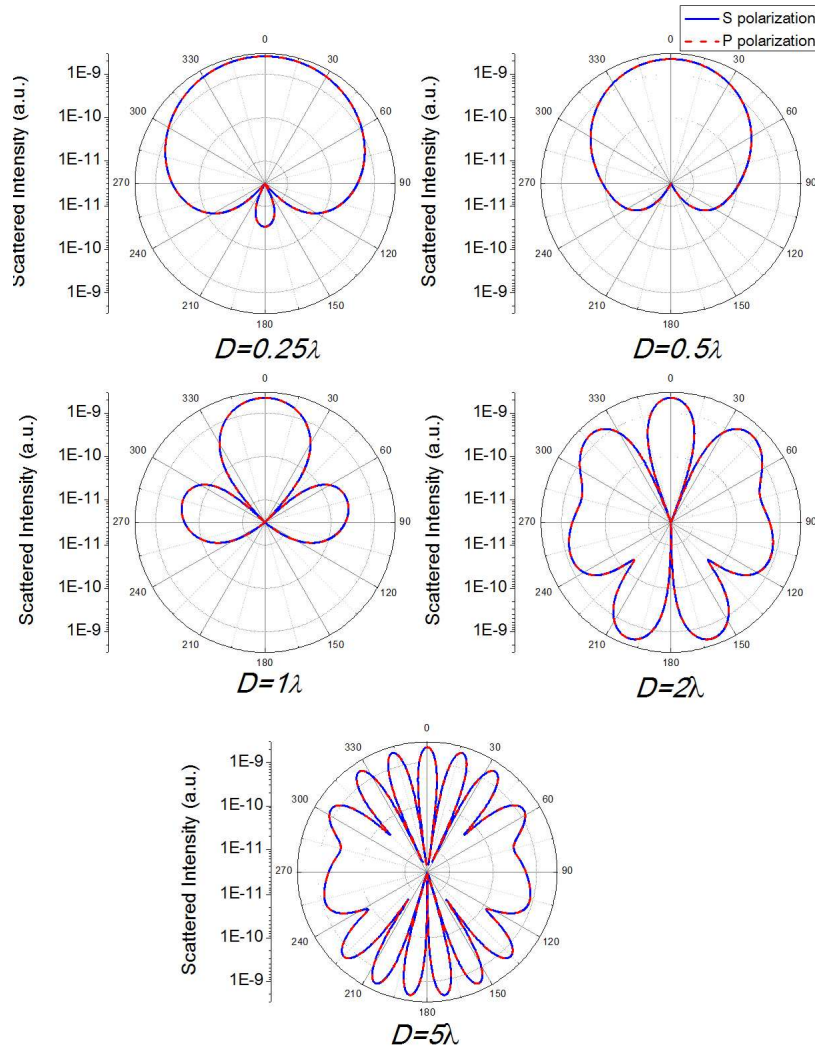
Fig. 4. Polar distribution of light scattering by an array similar to that described in Fig. 1d) for several distances between the particles. Both polarizations, parallel (P) and perpendicular (S) to the scattering plane, are considered. The distances are expressed in wavelength units.
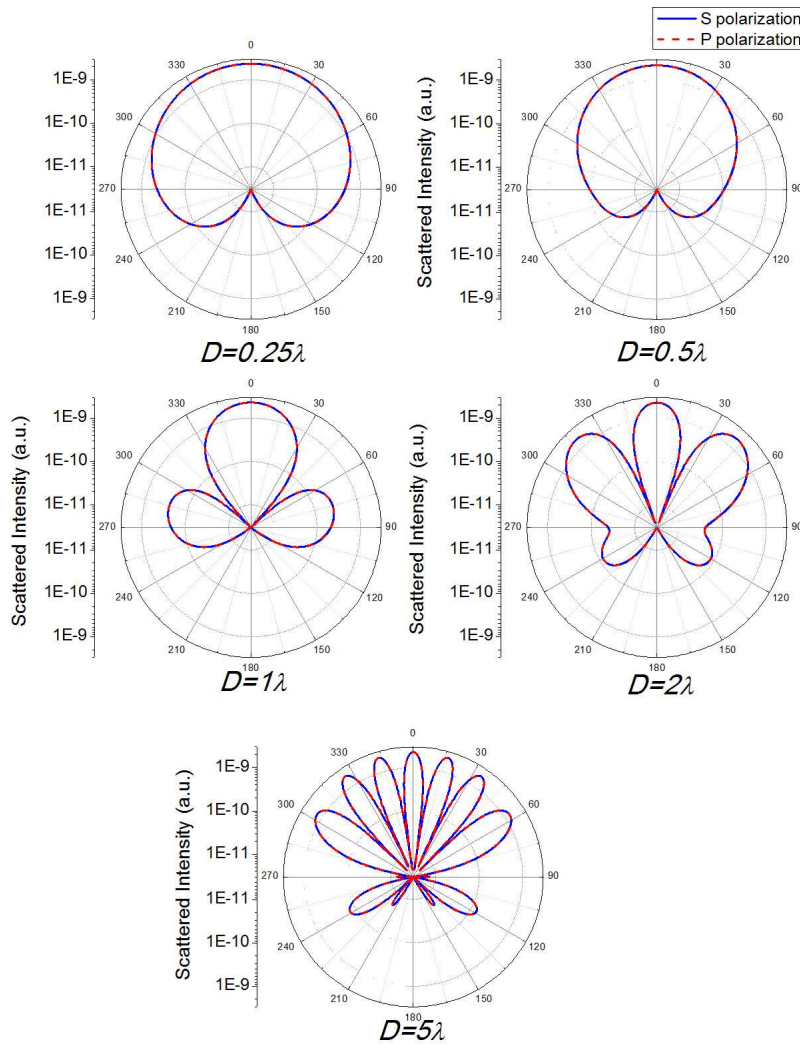
Fig. 5. Polar distribution of light scattering by an array similar to that described in Fig. 1f) for several distances between the particles. Both polarizations, parallel (P) and perpendicular (S) to the scattering plane, are considered. The distances are expressed in wavelength units.

Alignment tolerances are probably the main challenge that will arise in a future experimental implementation of this system. In order to analyze this issue, we have considered in-plane rotations of the array around an axis parallel to the incident direction which crosses the system through the centre of the square. In Fig. 6 we plot, using semi-logarithmic axes, the scattered intensity for such different systems with different rotations of the array (see inset). The incident light is polarized with the electric field perpendicular to the scattering plane (S polarization) and the diagonal of the square is $D = 0.25\lambda$. As the electric and magnetic contributions are compensated in these configurations, S and P polarizations produce similar results. It can be seen that the minimum backscattering still appears for any rotation of the system. This means that the observation of the minimum in the back-scattered light is independent of the position of the array in the normal plane. Only small differences are observed for scattering angles around 90° and 270°. These differences are due to the different environment that the electric field sees at those angles. For example, when the rotation angle is 0°, the electric field doesn't see any particle in scattering plane at 90° or 270°, but under a

45° rotation, the incident electric field sees an electric particle at these angles (see inset in Fig. 6).
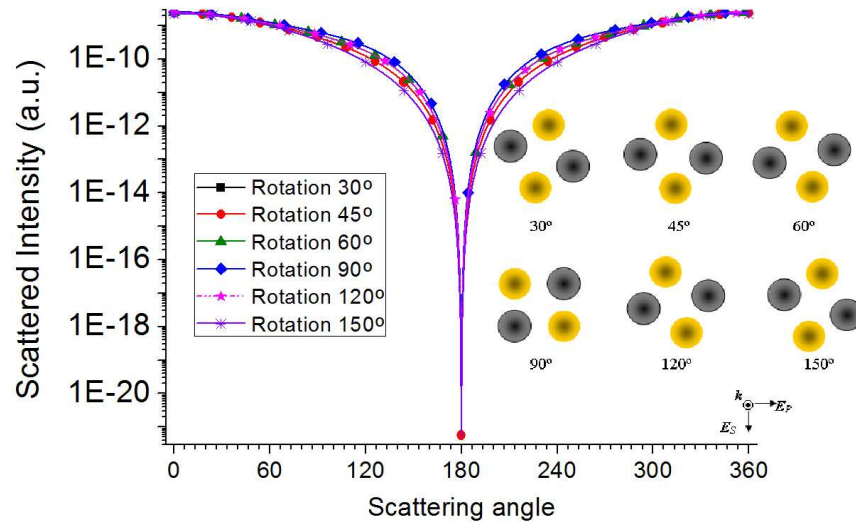

Fig. 6. Scattered intensity for different rotations of the original array around an axis parallel to the incident direction. The incident wave has S polarization. The rotation of the system is described in the inset.

3. Extensions of the alternate-array

The particle configuration described in the previous section can be used as cell to generate a larger composed from electric and magnetic particles that follow the arrangement described in Fig. 1f). As an example, we analyse an array with 16 electric and magnetic particles placed alternatively, as shown in Fig. 7. As before, the system is illuminated with a linearly polarized plane wave and both polarizations (perpendicular and parallel to the scattering plane) are considered. Also, as in the previous case, we use the diagonal of the square as a geometrical parameter to characterize the configuration.

The light scattering patterns for the geometry in Fig. 7 and for different distances between the particles is shown in Fig. 8. We observe that the sharp minimum in the backward scattered light is still present for every particle distance. Also, as before, the angular range at which the minimum of the scattered intensity in the backward direction can be observed slightly depends on the particle distances. For distances equal to $\lambda/2$ and λ the minimum is observed in a range of 120° around 180°, while this range decreases to 60° for the other geometries. The larger number of particles produces a stronger diffraction interaction between the particles and leads to a larger number of lobes in the scattering patterns than when we considered 4 particles (compare Figs. 5 and 8).
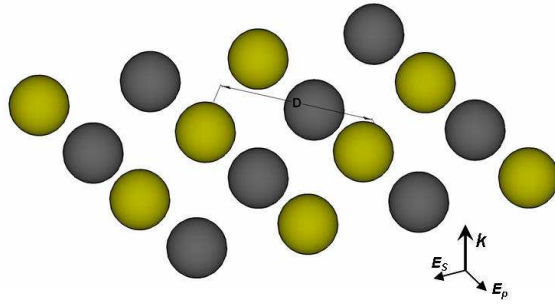
Fig. 7. Schematic of an array with 16 electric (dark) and magnetic (yellow) nanoparticles ($R = 0.01\lambda$) following the alternate configuration.
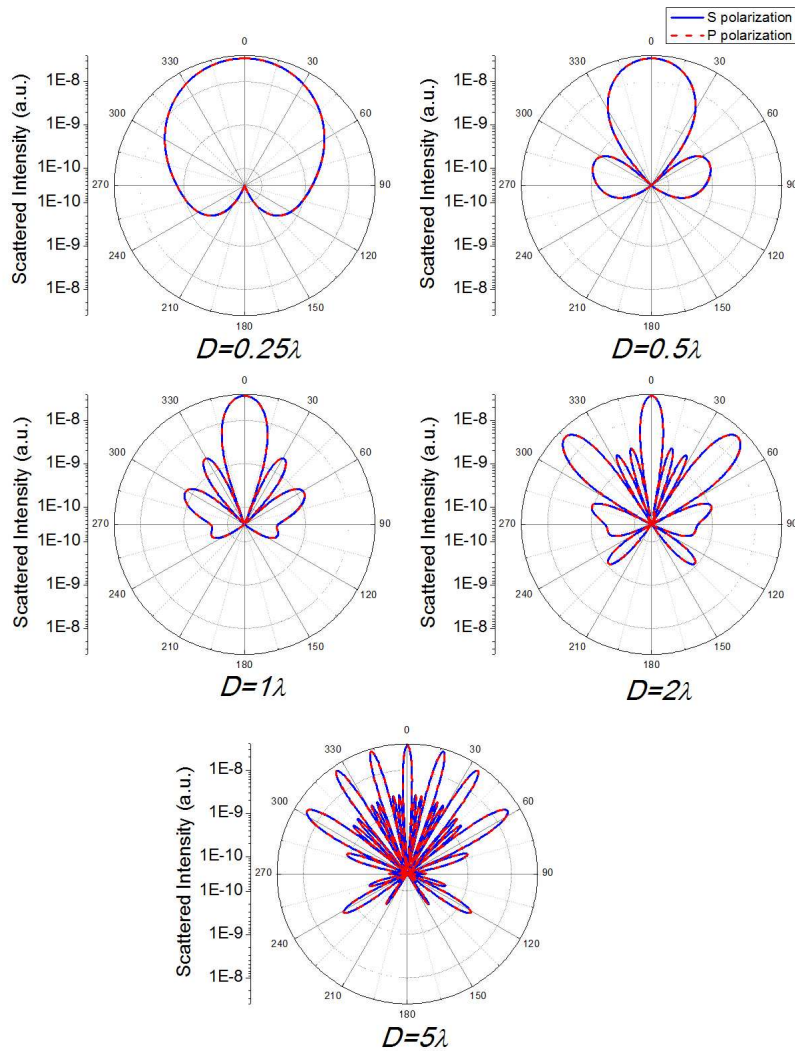

Fig. 8. Scattering patterns, for both polarizations, corresponding to the 16-particle array configuration shown in Fig. 7. The distances between particles D are in wavelength units

In Fig. 9, we show in a semi-logarithmic plot the intensity scattered by the array of 16 particles with $D = 0.25\lambda$, as a function of the scattering angle and for several rotations of the system around an axis parallel to the incident direction. As was the case for the smaller array, any rotation of the configuration does not produce a remarkable change in the backward direction, and the minimum in that direction still appears clearly. This insensitivity to the structure alignment is a very important and helpful characteristic for the experimental design and future applications of this kind of systems. For the large array, the scattered intensity is less sensitive to any rotation of the system than the 4-particles array; a difference can only be observed for scattering angles in the range *[90° <θ <160°].*
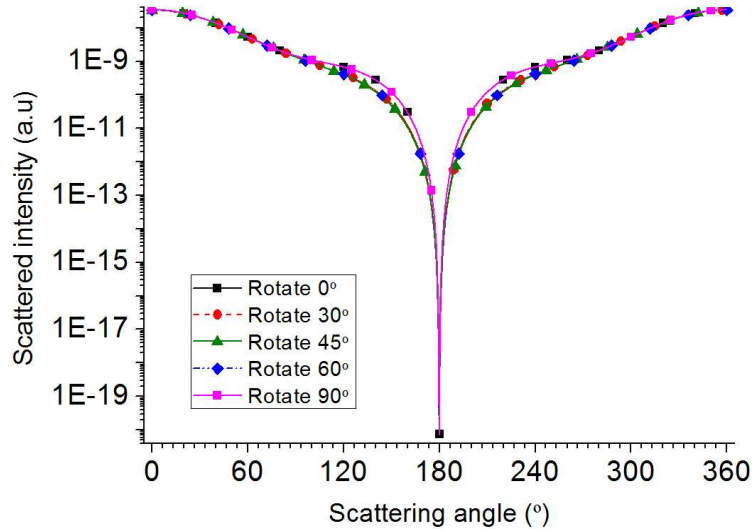

Fig. 9. Scattered intensity for an alternate array of 16 particles (D = 0.25λ) a function of the scattering angle and for different rotations of the system around an axis parallel to the incident direction. The incident wave is considered with S polarization.

The larger an array, the higher the risk to position a particle inaccurately. The physical behaviour exploited in this work is based on the fact that the electric and magnetic contributions to light backscattering by different particles are compensated. One placement error in the array, e.g. changing one electric particle with a magnetic one or vice versa, displacing one of the particles, or even removing one or more particles from the array, lead to the fact that this compensation disappear. As an example, in Fig. 10, the scattered intensity is plotted as a function of the scattering angle for an ideal array of 16 particles and for some possible experimental errors: a) on the particle's properties, b) on the position of the particles and even c) when one or more particles are removed from the array.

The results in Fig. 10 indicate that a simple error in the array pretty much destroys the minimum in the backward scattering. The fact that the scattering for both polarizations is equal also disappears when an error is included in the array (results are only shown for one polarization in Fig. 10 for space reasons).
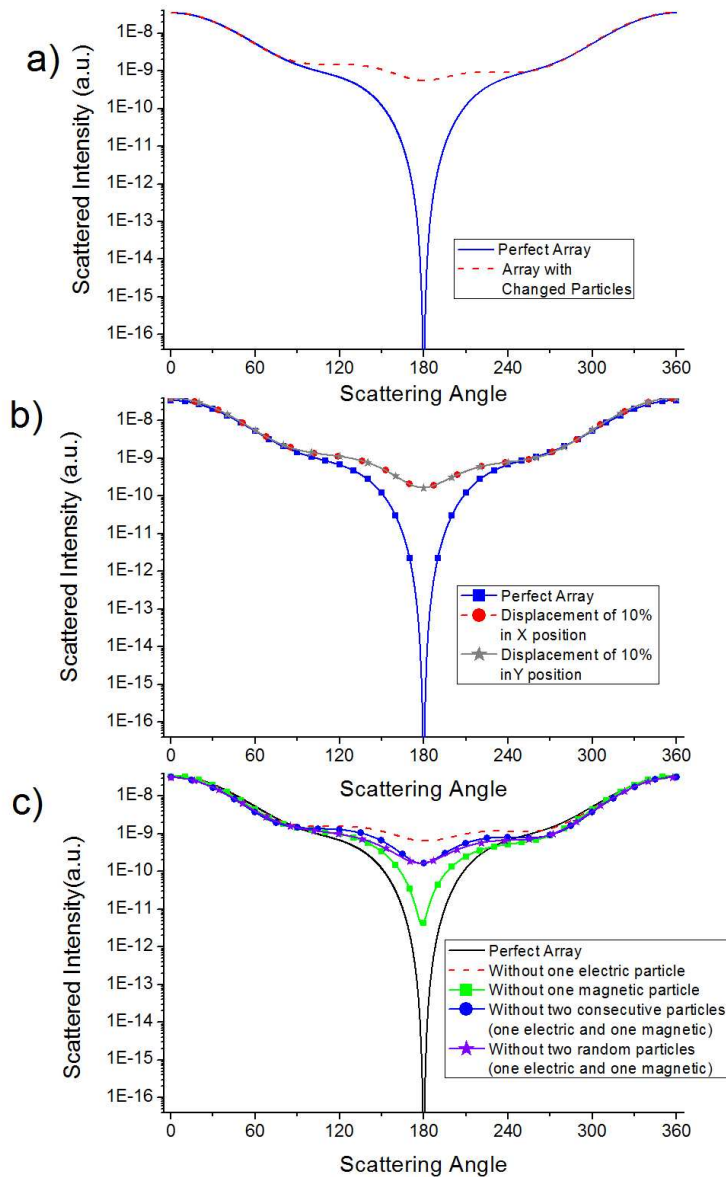
Fig. 10. Comparison of the scattered intensity for a 16-particle array with and without placing errors. Different kinds of errors are considered a) changing an electric particle for a magnetic one, b) displacing one of the particles of the array and c) eliminating one or more particles of the array. P- polarization is used. The distance between the particles is $D = 0.25\lambda$.

Another very interesting extension of the system consists in considering more than one layer [30]. This kind of array can be produced by stacking several layers with similar or different configurations. In this work, we consider two cases: two arrays of 16 particles one above the other with a spacing d, and either both with a configuration equal to that shown in Fig. 7 or with complementary configurations (at the same position of a magnetic particle in the bottom layer, there is an electric one in the top array and vice versa). A typical result is shown in Fig. 11 where we report the scattering intensity, in semi-logarithmic scale, as a function of the scattering angle for the two-equal-arrays case and for S polarization. As can be seen the absence of backscattering is still observed in this case. Even when the two layers are

different, the electric and magnetic contributions are compensated and the scattering pattern is very similar to that shown in Fig. 11. The minimum of the scattered intensity in the backward direction is independent on the inter-particle (D) and inter-layer (d) distances. The influence of the distance is observed for other scattering angles because more interferential lobes appear when the distance increases. This geometry is also independent to the polarization, and a P polarization illumination produces the same results.
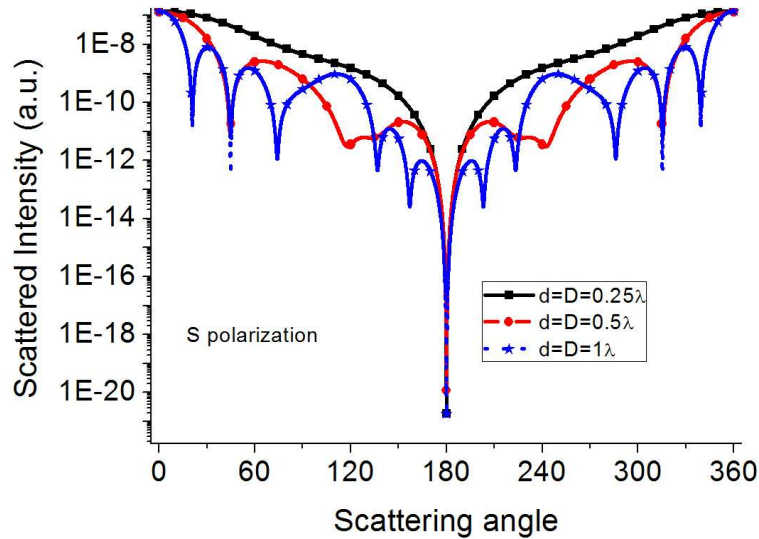

Fig. 11. Scattered intensity as a function of the scattering angle for a system composed of two arrays like in Fig. 7, on top of each other. The incident field is S polarized and different distances between the particles (D) and layers (d), expressed in wavelength units, are considered.

In a previous work [10] we have analyzed the size effects on the directional scattering behavior for nanoparticles with electric and magnetic optical properties fulfilling Kerker' conditions. In that work, we concluded that the minima in the scattered intensity in the backward or forward direction depend on the particle size. As the radius R increases, the minimum is less pronounced and the pairs (ε,μ) at which it appears change slightly. Since the proposed array behaves as one of those particles, we can suppose that the influence of the size on the scattering patterns of the array will be similar and, as particles of the array become larger, the minimum in the scattered intensity at backward direction becomes less abrupt.

5. Conclusions

Over the last years, the interest in special scattering properties and in new metamaterials has increased exponentially, opening new and interesting applications in several fields, including medicine, technological industry or communications. Recently, plasmonic magnetic particles have been developed experimentally [22] but in spite of important efforts in the design and manufacturing of metamaterials, it is not yet possible to obtain nanoparticles with both electric and magnetic properties negative and resonant.

In this work, we overcome this limitation by proposing a geometrical configuration consisting of an array of electric ($\varepsilon = -2.01, \mu = 1$) and magnetic ($\varepsilon = 1, \mu = -2.01$) nanoparticles. Such an array presents similar scattering properties to those of an isolated particle of the same radius with double negative optical constants ($\varepsilon = \mu = -2.01$). The light scattered by a particle with these optical constants exhibits extremely interesting features: a double dipolar resonance, one electric plus one magnetic, and a minimum in the backscattered

intensity. We have demonstrated that for a specific geometrical configuration called "alternate" configuration, a minimum backscattering can be observed for an array of particles including a few or a large number of particles. This minimum backscattering is independent of the inter-particle distance and of any rotation of the array in the plane, which should make its fabrication very robust. In addition, the lack of scattered intensity in the backward direction persists, even when more than one layer is considered.

Since double-negative materials are still difficult to fabricate nowadays, we believe that the structures investigated in this publication can propose a feasible alternative in order to generate materials with a double-negative behavior to develop new and interesting devices, techniques or treatments based on their unusual scattering properties.

Acknowledgements